Supporting Information

Novel Low-Temperature Process for Perovskite Solar Cells with a Mesoporous TiO_2 Scaffold

Patricia S.C. Schulze,[*,†,‡] *Alexander J. Bett,*[†,‡] *Kristina Winkler,*[†] *Andreas Hinsch,*[†] *Seunghun Lee,*[†] *Simone Mastroianni,*[†,‖] *Laura E. Mundt,*[†] *Markus Mundus,*[†] *Uli Würfel,*[†,‖] *Stefan W. Glunz,*[†,⊥] *Martin Hermle,*[†] *and Jan Christoph Goldschmidt*[†]

[†] Fraunhofer Institute for Solar Energy Systems, Heidenhofstrasse 2, 79110 Freiburg, Germany

[‖] Freiburg Materials Research Center (FMF), Albert-Ludwigs-University of Freiburg, Stefan-Meier-Strasse 21, 79104 Freiburg, Germany

[⊥] Freiburg Center for Interactive Materials and Bioinspired Technologies (FIT), Albert-Ludwigs-University of Freiburg, Georges-Köhler-Allee 105, 79110 Freiburg, Germany

* email: patricia.schulze@ise.fraunhofer.de

[‡] P.S.C.S. and A.J.B. contributed equally to this work

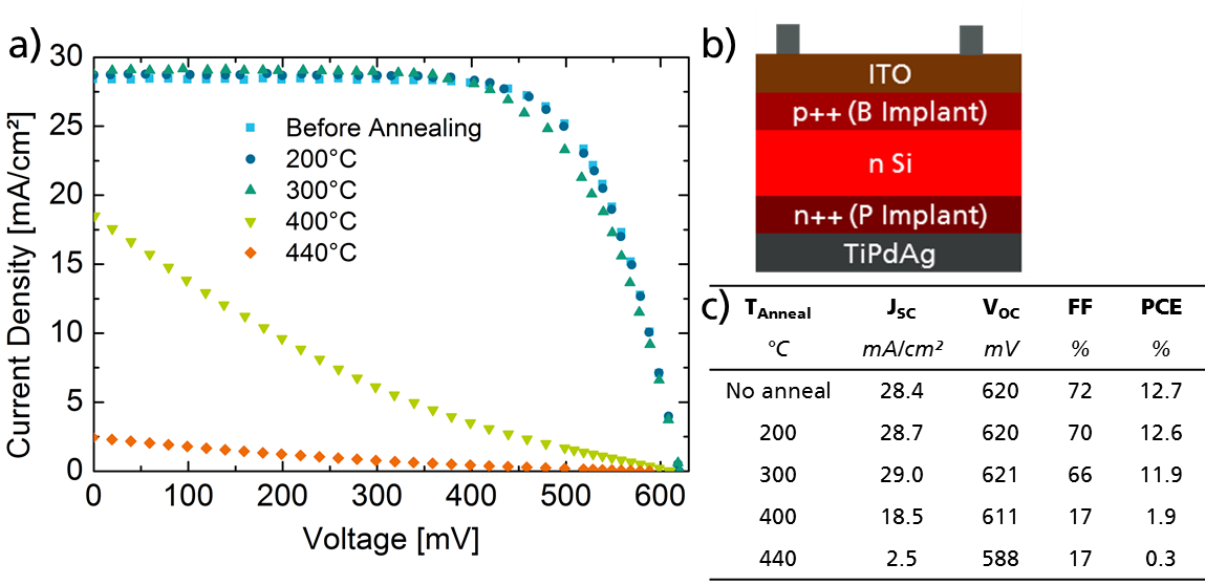

c)

T_{Anneal}	J_{SC}	V_{OC}	FF	PCE
°C	*mA/cm²*	*mV*	%	%
No anneal	28.4	620	72	12.7
200	28.7	620	70	12.6
300	29.0	621	66	11.9
400	18.5	611	17	1.9
440	2.5	588	17	0.3

Figure S1. a) IV curves of silicon solar cells with ITO as a front layer measured after annealing at different temperatures (each 60 min). b) Sketch of the investigated solar cells. c) Parameters corresponding to the IV curves. Solar cells were fabricated on n type silicon (1 Ω cm). A phosphorous back surface field and a boron emitter were implanted at the rear and front sides, respectively. Afterwards, a 70 nm thick ITO layer was sputtered on top of the emitter. Rear side metallization was realized by successive evaporation of 50 nm of titanium, 50 nm of palladium and 1000 nm of silver (TiPdAg). At the front, a silver contact grid was thermally evaporated. Temperatures over 400 °C like in the high-T perovskite process damage the silicon bottom solar cell. Additional resistance measurements on silicon substrates coated with ITO show that the interface between silicon and ITO does not stand this high temperatures. Hence, in tandem solar cells ITO can only be used as an interconnection layer when the perovskite top solar cell is produced by a low-T process.

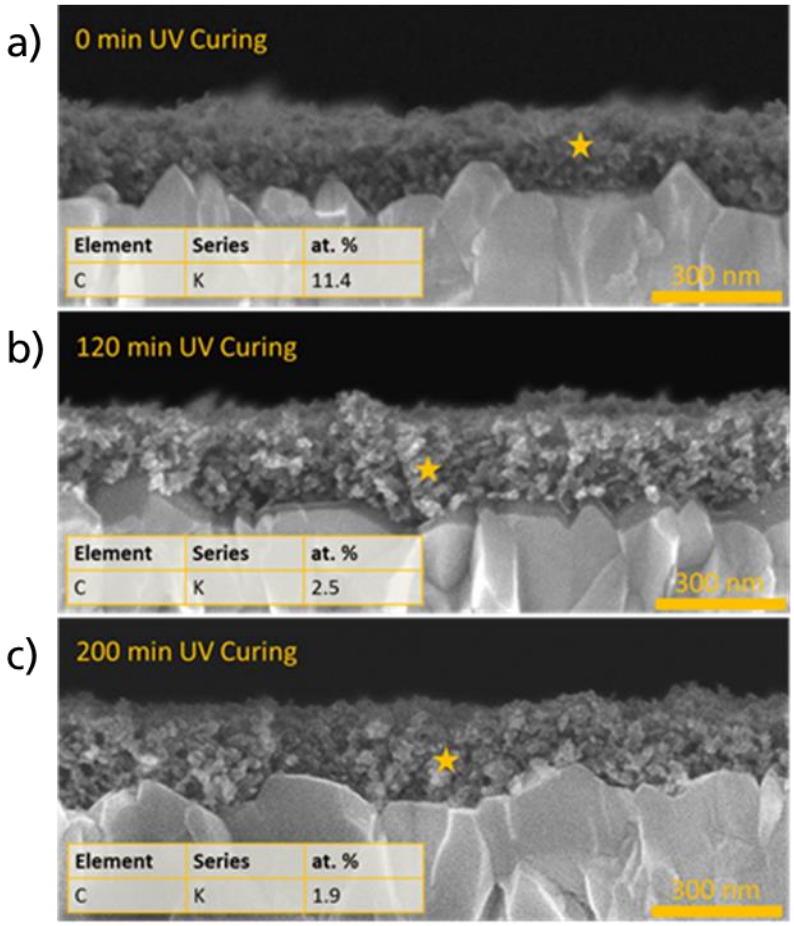

Figure S2. Scanning electron microscopy cross-sectional images of the mp-TiO_2 layer on a FTO-coated glass substrate a) as deposited without UV treatment, b) after 120 min and c) 200 min of UV treatment. Stars mark the position of EDX analysis. The carbon contents determined from EDX spectra depict the trend of effective removal of organic paste components by UV curing. The difference between 120 min and 200 min lies within the uncertainty of the measurement. In the case of b) an intermediate layer of 20 nm c-TiO_2 was deposited. The layer evenly covers the rough FTO surface.

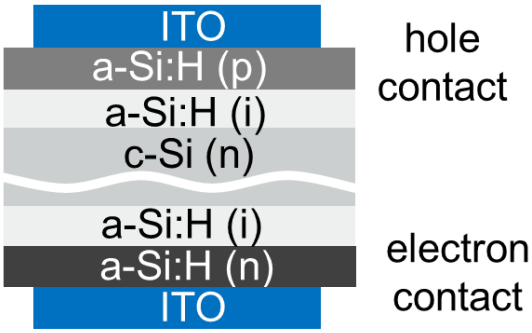

Figure S3. Sketch of a silicon heterojunction precursor, which could serve as bottom solar cell (with additional rear metallization) in a perovskite silicon tandem device. On such precursors, the impact of UV curing of 200 min was tested. The stack consists of a n-doped crystalline silicon wafer with intrinsic (i) and doped (p and n) hydrogenated amorphous silicon (a-Si:H) layers covered with indium doped tin oxide (ITO) on both sides. Quasi steady-state photoconductance (QSSPC) measurements showed an implied V_{OC} and implied *FF* of around 720 mV and 84%, respectively, for as made samples. No significant change in these values was observed after UV curing. The same value for implied V_{OC} was obtained from SunsV_{OC} measurements, before and after UV curing. Furthermore, in the case of tandem solar cell fabrication, the compact and mesoporous TiO_2 layers would be present on the ITO during the UV curing, which would further reduce UV light exposure of the silicon solar cell during curing. Therefore, one can conclude that the low-T route is applicable for perovskite silicon tandem solar cells.

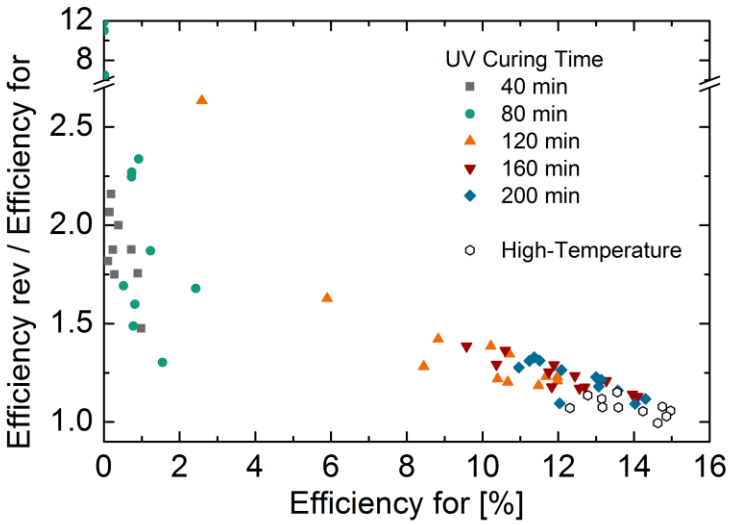

Figure S4. Relative enhancement of reverse scan direction efficiency (Efficiency rev / Efficiency for) as a function of the forward scan direction efficiency (Efficiency for). A clear trend can be seen; with increasing solar cell performance, the hysteresis decreases.

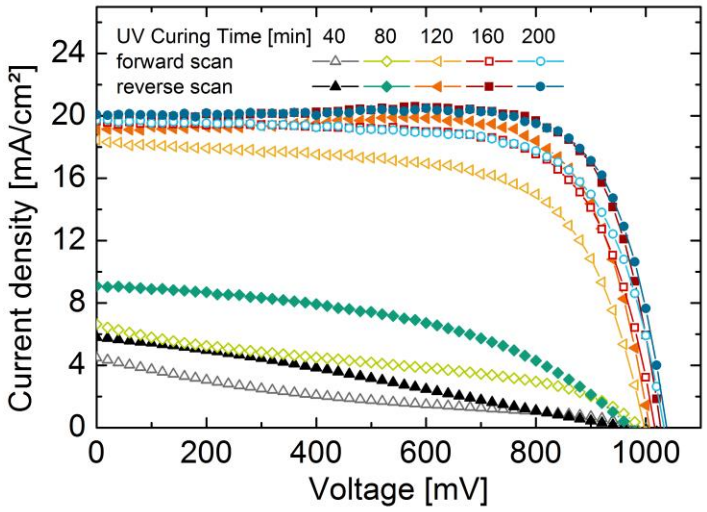

Figure S5. Current-voltage (IV) curves of the best cell of each UV curing time corresponding to the data represented in Table S1.

Table S1. Solar cell performance parameters corresponding to Figure 3. For different UV curing times the mean values of J_{SC}, V_{OC}, *FF* and efficiency obtained from the indicated number of solar cells are represented for the forward and reverse scan directions, respectively. The appropriate values are also shown for the best cell. The best cell is defined as the cell with the highest efficiency mean value obtained from efficiencies of forward and reverse scan directions.

UV curing time			J_{SC} [mA cm^{-2}]	V_{OC} [mV]	FF [%]	Efficiency [%]
40 min	Mean (9 cells)	for	2.4 ± 1.3	884 ± 93	20 ± 4	0.4 ± 0.3
		rev	3.0 ± 1.6	849 ± 91	30 ± 8	0.8 ± 0.5
	Best cell	*for*	*4.5*	*971*	*20*	*0.9*
		rev	*5.8*	*990*	*28*	*1.6*
80 min	Mean (12 cells)	for	3.2 ± 2.2	899 ± 155	24 ± 7	0.8 ± 0.7
		rev	4.5 ± 2.9	910 ± 90	34 ± 6	1.5 ± 1.1
	Best cell	*for*	*6.7*	*987*	*37*	*2.4*
		rev	*9.1*	*973*	*46*	*4.1*
120 min	Mean (12 cells)	for	16.2 ± 2.8	979 ± 34	59 ± 9	9.6 ± 2.7
		rev	17.3 ± 2.4	995 ± 32	72 ± 3	12.6 ± 2.3
	Best cell	*for*	*18.5*	*994*	*65*	*12.0*
		rev	*19.1*	*1006*	*77*	*14.7*
160 min	Mean (12 cells)	for	18.3 ± 0.9	994 ± 19	66 ± 4	12.1 ± 1.3
		rev	19.0 ± 0.8	1009 ± 17	77 ± 2	14.8 ± 0.9
	Best cell	*for*	*19.6*	*1014*	*71*	*14.1*
		rev	*19.9*	*1026*	*78*	*15.9*
200 min	Mean (12 cells)	for	19.0 ± 0.7	1003 ± 16	66 ± 3	12.5 ± 1.1
		rev	19.6 ± 0.5	1017 ± 15	76 ± 4	15.2 ± 0.8
	Best cell	*for*	*19.8*	*1030*	*70*	*14.3*
		rev	*20.1*	*1036*	*77*	*16.0*
High-T	Mean (11 cells)	for	19.6 ± 0.6	983 ± 25	72 ± 1	13.8 ± 0.9
		rev	19.8 ± 0.5	1007 ± 26	74 ± 1	14.9 ± 0.8
	Best cell	*for*	*20.2*	*1020*	*73*	*15.0*
		rev	*20.2*	*1041*	*75*	*15.8*

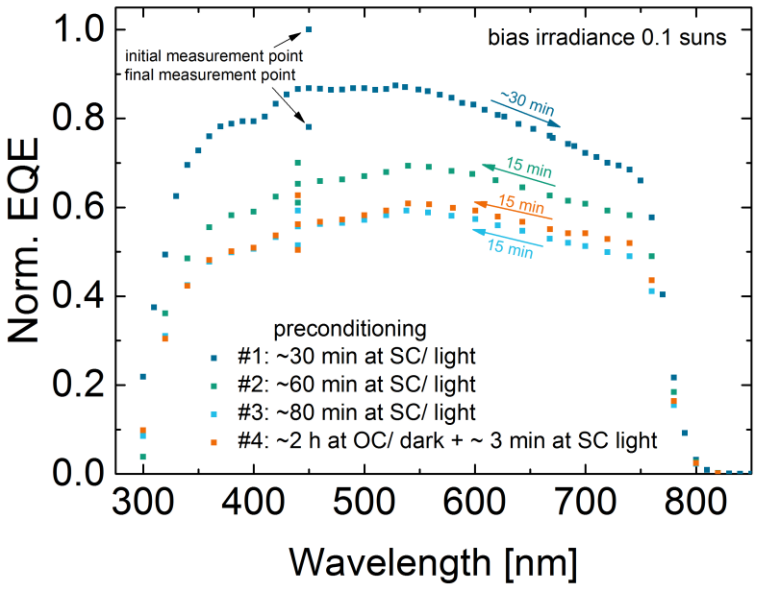

Figure S6. External quantum efficiencies (EQEs) of a perovskite solar cell fabricated by the low-T process with 120 min of UV curing normalized to the maximum value of the first EQE measurement (#1). To investigate the observed decrease in J_{SC} during the measurement under illumination at short-circuit conditions, EQE measurements were repeated after preconditioning under elongated periods of short-circuit conditions. Chopping frequency was 70 Hz. The scan duration is noted next to the arrow indicating the scan direction. An EQE measurement at one wavelength was repeated before and after the EQE scan marked as initial and final measurement point in the graph. They show that during each measurement under short-circuit conditions the cell's performance decreases. This is more pronounced for the longer scan duration of 30 min. Conducting the measurement from both wavelength scan directions, it is shown that this decrease is independent of the wavelength scan direction. With ongoing measurement duration increasing underestimation of the EQE might occur. Repeating the measurements after keeping the cell illuminated at short circuit conditions, the EQE continues to drop. However, the shape stays the same comparing measurements with the same scan direction (#2, #3, #4) independent of the

preconditioning. Slight recovery could be observed after keeping the cell for 2 h in the dark at open-circuit voltage. We therefore conclude that the observed effect of performance decrease is at least partially reversible and might relate to ion migration or charge carrier trapping at defects also responsible for hysteresis.[1] Moreover, these results underline that the reliability of EQE measurements should always be checked and that a comparison of integrated J_{SC} from EQE measurements with J_{SC} from IV scans is difficult for cells with such dynamic behavior at short-circuit conditions.

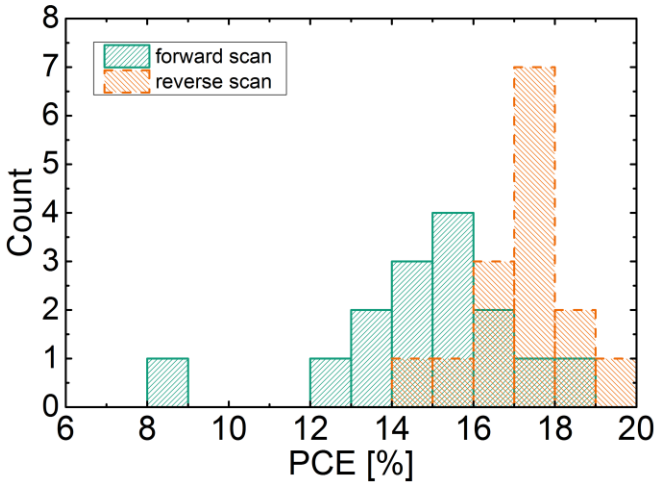

Figure S7. Histogram of the measured efficiency values of one batch of 15 solar cells produced with the low-T process, containing the record solar cell. Efficiencies were extracted from forward and reverse IV-scan direction, respectively.

REFERENCES

(1) Elumalai, N. K., Uddin, A. Hysteresis in Organic-Inorganic Hybrid Perovskite Solar Cells. *Sol. Energ. Mat. Sol. C.* **2016**, *157*, 476-509.